

# A hydrogel-based model of aortic stiffness reveals that microtubules are novel regulators of smooth muscle cell hypertrophy

Robert Johnson<sup>1</sup>, Sultan Ahmed<sup>1</sup>, Finn Wostear<sup>1</sup>, Christopher Morris<sup>1</sup>, and Derek Warren<sup>1</sup>

<sup>1</sup>University of East Anglia

November 29, 2022

## Abstract

Decreased aortic compliance is a precursor to numerous cardiovascular diseases. Compliance is regulated by the stiffness of the aortic wall and the vascular smooth muscle cells (VSMCs) within it. During ageing, the extracellular matrix of the aortic wall stiffens, reducing compliance and leading to conditions such as hypertension. In response, VSMCs generate enhanced contractile forces and undergo hypertrophy, promoting VSMC stiffening and further reducing compliance. Due to a lack of suitable in vitro models, the mechanisms driving VSMC hypertrophy in response to matrix stiffness remain poorly defined. Human VSMCs were seeded onto polyacrylamide hydrogels whose stiffness mimicked either healthy or aged/diseased aortae. VSMC response to contractile agonist stimulation was measured through changes in cell area and volume. VSMCs were pre-treated with pharmacological agents prior to agonist stimulation to identify regulators of VSMC contractility and hypertrophy. VSMCs undergo a differential response to contractile agonist stimulation based on matrix stiffness. On pliable hydrogels, VSMCs contract, decreasing in cell area whereas on rigid hydrogels, VSMCs undergo a hypertrophic response, increasing in area and volume. Microtubule stabilisation prevented hypertrophy whilst leaving VSMC contraction on pliable hydrogels unimpeded. Conversely, microtubule destabilisation inhibited contraction and induced hypertrophy within VSMCs on pliable hydrogels. In response to enhanced matrix rigidity, VSMC undergo a hypertrophic response as result of decreased microtubule stability. Using standard biological techniques and equipment, we present a screening assay capable of identifying novel regulators of matrix rigidity induced VSMC hypertrophy. This assay can identify both beneficial and deleterious effects of pharmacological agents to cardiovascular health.

## A hydrogel-based model of aortic stiffness reveals that microtubules are novel regulators of smooth muscle cell hypertrophy

*Running Title:* Microtubules regulate smooth muscle cell hypertrophy

**Robert T. Johnson<sup>1+</sup>, Sultan Ahmed<sup>1</sup>, Finn Wostear<sup>1</sup>, Christopher J. Morris<sup>1,2</sup> and Derek T. Warren<sup>1+</sup>**

<sup>1</sup> School of Pharmacy, University of East Anglia, Norwich Research Park, Norwich, United Kingdom.

<sup>2</sup> School of Pharmacy, University College London, London, United Kingdom.

+ Corresponding Author(s): Dr. Robert Johnson (robert.johnson@uea.ac.uk) &

Dr. Derek Warren (derek.warren@uea.ac.uk) School of Pharmacy, University of East Anglia, Norwich Research Park, Norwich, Norfolk, UK, NR4 7TJ

*ORCID IDs:* RTJ (<https://orcid.org/0000-0003-3618-238X>)

CJM (<https://orcid.org/0000-0002-7703-4474>)

DTW (<https://orcid.org/0000-0003-0346-7450>)

*Word Count:* 2,740

*Data Availability:* The data that support the findings of this study are available from the corresponding author upon reasonable request.

*Funding Statement:* This work was funded by a Biotechnology and Biological Sciences Research Council Research Grant (BB/T007699/1) and a British Heart Foundation PhD Studentship (FS/17/32/32916) awarded to DTW and a UKRI Biotechnology and Biological Sciences Research Council Norwich Research Park Doctoral Training Partnership PhD Studentship awarded to FW.

*Author Contributions:* RTJ, SA and FW were responsible for performing experiments and analysing data. DTW analysed data. CJM reviewed and edited this manuscript. RTJ and DTW were responsible for the design, writing and editing of this manuscript.

*Conflict of Interests:* The authors declare that the research was conducted in the absence of any commercial or financial relationships that could be construed as a potential conflict of interest.

*Abstract*

**Background and Purpose:** Decreased aortic compliance is a precursor to numerous cardiovascular diseases. Compliance is regulated by the stiffness of the aortic wall and the vascular smooth muscle cells (VSMCs) within it. During ageing, the extracellular matrix of the aortic wall stiffens, reducing compliance and leading to conditions such as hypertension. In response, VSMCs generate enhanced contractile forces and undergo hypertrophy, promoting VSMC stiffening and further reducing compliance. Due to a lack of suitable *in vitro* models, the mechanisms driving VSMC hypertrophy in response to matrix stiffness remain poorly defined.

**Experimental Approach:** Human VSMCs were seeded onto polyacrylamide hydrogels whose stiffness mimicked either healthy or aged/diseased aortae. VSMC response to contractile agonist stimulation was measured through changes in cell area and volume. VSMCs were pre-treated with pharmacological agents prior to agonist stimulation to identify regulators of VSMC contractility and hypertrophy.

**Key Results:** VSMCs undergo a differential response to contractile agonist stimulation based on matrix stiffness. On pliable hydrogels, VSMCs contract, decreasing in cell area whereas on rigid hydrogels, VSMCs undergo a hypertrophic response, increasing in area and volume. Microtubule stabilisation prevented hypertrophy whilst leaving VSMC contraction on pliable hydrogels unimpeded. Conversely, microtubule destabilisation inhibited contraction and induced hypertrophy within VSMCs on pliable hydrogels.

**Conclusions and Implications:** In response to enhanced matrix rigidity, VSMC undergo a hypertrophic response as result of decreased microtubule stability. Using standard biological techniques and equipment, we present a screening assay capable of identifying novel regulators of matrix rigidity induced VSMC hypertrophy. This assay can identify both beneficial and deleterious effects of pharmacological agents to cardiovascular health.

*Keywords:* Contraction, Hypertrophy, Matrix Stiffness, Microtubules, Microtubule Stability, Polyacrylamide Hydrogel, Vascular Smooth Muscle Cell (VSMC)

*Introduction*

Aortic compliance describes the ability of the aorta to change shape in response to changes in blood pressure. Maintaining aortic compliance is essential for cardiovascular (CV) health and decreased aortic compliance is a major risk factor associated with a variety of age-related CV diseases (Glasser et al., 1997; Mitchell et al., 2010; Lacolley et al., 2020). Aortic compliance can be measured clinically by pulse wave velocity (PWV) and increased PWV is associated with increased CV mortality (Cruickshank et al., 2002; Safar et al., 2002; Zhong et al., 2018; Sequí-Domínguez et al., 2020). The rigidity of the aortic wall is a major contributor to aortic compliance. In the healthy aortic wall, rigidity and compliance are determined by the balance between elastic-fibres, including elastin, which provides pliability, and non-elastic fibres, including collagen-I that

provides tensile strength to the extracellular matrix (ECM) (Tsamis et al., 2013). However, during ageing and CV disease, elastic-fibres degrade, and collagen-I accumulates. These ECM changes increase the rigidity of the aortic wall and decrease aortic compliance (Ahmed and Warren, 2018).

Aortic tone is regulated by the contraction of vascular smooth muscle cells (VSMC), the predominant cell type within the aortic wall (Leloup et al., 2019). Importantly, VSMC stiffness also contributes to aortic wall rigidity and increased VSMC stiffness further decreases aortic compliance in ageing and CV disease (Qiu et al., 2010; Sehgel et al., 2015b; Lacolley et al., 2017). In healthy aortae, wall rigidity and compliance are a balance between ECM rigidity and VSMC stiffness (Johnson et al., 2021). However, this balance is disrupted in ageing and CV disease, resulting in VSMC dysfunction (Sazonova et al., 2011; Lacolley et al., 2017). For example, in response to hypertension, VSMCs undergo a process known as hypertrophy and increase their cell mass without increasing cell number (Owens and Schwartz, 1983; Rizzoni et al., 2000; Zhang et al., 2005; Schiffrin, 2012). VSMC hypertrophy is known to increase aortic wall thickness and rigidity, and decrease aortic compliance (Zieman et al., 2005; Hayashi and Naiki, 2009; Sehgel et al., 2015a). However, mechanisms driving VSMC hypertrophy remain poorly defined. A major hindrance to understanding these processes has been the use of tissue culture plastic and glass, materials whose stiffness is around a thousand times greater than healthy aortae (Minaisah et al., 2016). In this study, we used polyacrylamide hydrogels to model healthy and diseased aortic rigidity. We demonstrate that enhanced matrix rigidity promotes contractile agonist stimulated VSMCs to undergo hypertrophy. Furthermore, we present a pharmacological screening assay through which novel regulators of VSMC hypertrophy can be identified. This assay can be performed with standard cell biological training and equipment, and has the capability to not only identify novel therapeutics, but allows for mechanistic hypotheses to be tested. Finally, we demonstrate that microtubule instability is a critical driver of VSMC hypertrophy.

## Methods

### 2.1 Polyacrylamide Hydrogel Preparation

Hydrogels were prepared as described previously (Minaisah et al., 2016). Glass coverslips were activated by treating with (3-Aminopropyl)triethoxysilane for two minutes, washed three times in dH<sub>2</sub>O, then fixed in 0.5% glutaraldehyde for 40 minutes. After fixation, coverslips were washed and left to air dry overnight. Polyacrylamide hydrogel buffer was comprised as follows: 12 kPa – 7.5% acrylamide, 0.15% bis-acrylamide in dH<sub>2</sub>O; 72 kPa – 10% acrylamide, 0.5% bis-acrylamide in dH<sub>2</sub>O. To prepare hydrogels for fabrication, the appropriate volume of buffer was supplemented with 10% APS (1:100) and TEMED (1:1,000) then placed on a standard microscopy slide and covered by an activated coverslip (13 mm coverslips required 30  $\mu$ l of supplemented buffer; 33 mm coverslips used 50  $\mu$ l). Once set, the hydrogels were washed three times in dH<sub>2</sub>O, crosslinked with sulfo-SANPAH (1:3,000) under UV illumination (365 nm) for five minutes, then functionalised with collagen I (0.1 mg ml<sup>-1</sup>) for ten minutes at room temperature. Hydrogel stiffnesses have previously been confirmed using a JPK Nanowizard-3 atomic force microscope (Porter et al., 2020).

### 2.2 Vascular Smooth Muscle Cell Culture

Human adult aortic VSMCs (passages 3-9) were purchased from Cell Applications Inc. (354-05a). Standard VSMC culture was performed as previously described (Ragnauth et al., 2010; Warren et al., 2015). VSMCs were seeded onto polyacrylamide hydrogels in basal media (Cell Applications Inc Cat# 310-500), 18 hours prior to the beginning of the experiment. Briefly, VSMCs were pre-treated with pharmacological agents for 30 minutes, prior to co-treatment with a contractile agonist for an additional 30 minutes. Experimental specific concentrations are provided in the corresponding figure legends. Please see **Supplementary Table S1** for details of compounds used in this study.

### 2.3 Immunofluorescence and VSMC Area/Volume Analysis

Cells were fixed in 4% paraformaldehyde for ten minutes, permeabilised with 0.5% NP40 for five minutes, then blocked with 3% BSA/PBS for one hour. Primary staining against lamin A/C (1:200) (Sigma-Aldrich Cat# SAB4200236, RRID:AB\_10743057) was performed overnight at 4 °C in 3% BSA/PBS. Secondary

staining was performed using the appropriate Alexa Fluor 488 antibody (1:400) (Thermo Fisher Scientific Cat# A-11001, RRID:AB\_2534069) in the dark for two hours. F-actin was visualised using Rhodamine Phalloidin (1:400) (Thermo Fisher Scientific Cat# R145). Images were captured at 20x magnification using a Zeiss LSM980-Airyscan confocal microscope. Cell area and volume was measured using FIJI, open-source software (Schindelin et al., 2012; Ahmed et al., 2022)

## 2.4 Traction Force Microscopy

VSMCs were seeded onto polyacrylamide hydrogels containing 0.5  $\mu\text{m}$  red fluorescent (580/605) FluoSpheres (1:1000) (Invitrogen). Following angiotensin II stimulation (30 minutes), cell lysis was achieved by the addition of 0.5% Triton X-100. Images were captured at 20x magnification before and after lysis at 2-minute intervals using a Zeiss Axio Observer live cell imaging system. Drift was corrected using the ImageJ StackReg plugin and traction force was calculated using the ImageJ FTTC plugin that measured FluoSphere displacement (Tseng et al., 2012). Briefly, bead displacement was measured using the first and last image of the movie sequence. The cell region was determined by overlaying the traction map with the phase image, selecting the cell traction region with an ROI and extracting the traction forces in each pixel using the XY coordinate function in FIJI (Porter et al., 2020; Ahmed et al., 2022).

## 2.5 Cold-Stable Microtubule Stability Assay

Cold-stable microtubules were identified as per previous studies (Atkinson et al., 2018). Following treatment, cells were placed on ice for 15 minutes before being washed once with PBS and twice with PEM buffer (80  $\mu\text{M}$  PIPES pH 6.8, 1 mM EGTA, 1 mM  $\text{MgCl}_2$ , 0.5% Triton X-100 and 25% (w/v) glycerol) for three minutes. Cells were fixed in ice-cold methanol for 20 minutes then blocked with 3% BSA/PBS for one hour. Microtubules were visualised by staining for  $\alpha$ -tubulin (1:200) (Cell Signalling Technology Cat# 3873, RRID:AB\_1904178) whilst cell nuclei were visualised using a DAPI containing mounting media. Images were captured at 40x magnification using a Zeiss AxioPlan 2ie microscope.

## 2.6 Cell Viability Assay

Cell viability was determined using a RealTime-Glo MT Cell Viability Assay, as per manufacturer's instructions. Briefly, 5,000 cells per well were seeded in a 96-well plate and exposed to a range of drug concentrations for one hour. Luminescence was subsequently measured using a Wallac EnVision 2103 Multilabel Reader (PerkinElmer).

## 2.7 Statistical Analysis

The data and statistical analysis in this study complies with the recommendations on experimental design and analysis in pharmacology (Curtis et al., 2018). Statistical analysis was performed using GraphPad Prism 6.05. Results are presented as mean  $\pm$  SEM, with individual data points shown. The number of independent repeats performed, and total number of cells analysed per experiment are detailed in the corresponding figure legend. Unpaired Student's *t*-tests were used for the comparison of two conditions. To compare more than two conditions a one-way ANOVA was performed, with either a Tukey's or Sidak's multiple comparison post-hoc test being performed as appropriate. Concentration-response curves are presented as mean  $\pm$  SEM plotted on a logarithmic scale. Log(agonist) vs response curves were generated using non-linear regression and subsequently used to derive  $\text{EC}_{50}$  and  $\text{IC}_{50}$  values. Comparisons between concentration ranges on different hydrogel stiffnesses were performed using a two-way ANOVA followed by Sidak's post-hoc test. Differences between conditions were considered statistically significant when  $P < 0.05$ .

## Results

### 3.1 Matrix stiffness alters isolated smooth muscle cell response to contractile agonist stimulation.

We set out to determine how enhanced matrix stiffness, akin to that of an aged/diseased aortic wall, would affect VSMC contraction. Quiescent VSMCs grown on pliable (12 kPa) or rigid (72 kPa) hydrogels were stimulated with increasing concentrations of the contractile agonist angiotensin II. Changes in VSMC area

were used as a measure of contractile response (Li et al., 1999; Wang et al., 2017; Halaidych et al., 2019; Ahmed et al., 2022). As previously observed, VSMCs on pliable hydrogels displayed a decrease in cell area as angiotensin II concentration increased (**Figure 1a, b & d**) (Ahmed et al., 2022). In contrast, VSMCs seeded on rigid hydrogels failed to undergo a contractile response (**Figure 1a, c & d**). VSMCs seeded on rigid hydrogels were initially smaller than those on pliable hydrogels, yet when exposed to increasing concentrations of angiotensin II, cell area increased (**Figure 1a & d**). Further analysis revealed a 10-fold increase in the angiotensin II  $EC_{50}$  value for VSMCs seeded on rigid compared to pliable hydrogels (**Figure 1d & Supplementary Table 1**). Stimulation of VSMCs with increasing concentrations of an alternative contractile agonist, carbachol, again resulted in a differential response whereby VSMC area was reduced on pliable hydrogels but increased on rigid hydrogels (**Figure 1e-h**). Carbachol  $EC_{50}$  values were comparable between the two stiffnesses (**Figure 1h & Supplementary Table 1**). Subsequent experiments were performed by stimulating VSMCs with 10  $\mu$ M of either angiotensin II or carbachol, a concentration which induced maximal area changes on both stiffnesses of hydrogel.

To confirm that the above changes were specific for receptor activation, we utilised receptor antagonists irbesartan and atropine. Irbesartan antagonises the angiotensin II type 1 receptor, AT1, whilst atropine antagonises acetylcholine receptors thereby blocking the effects of carbachol. Quiescent VSMCs grown on pliable or rigid hydrogels were stimulated with either angiotensin II or carbachol in the presence of an increasing concentration of their respective antagonist. On pliable hydrogels, increasing concentrations of irbesartan or atropine prevented VSMCs from undergoing a contractile response and decreasing in cell area (**Figure 2a, b, e & f**). Likewise, treatment with irbesartan or atropine prevented contractile agonist induced enlargement of VSMCs on rigid hydrogels (**Figure 2a, c, e & g**). Further analysis generated  $IC_{50}$  values of both antagonists on both stiffnesses of hydrogel (**Figure 2d, h & Supplementary Table 1**).

### **3.2 Isolated smooth muscle cells undergo a hypertrophic response on rigid substrates following contractile agonist stimulation.**

The above data demonstrates that matrix stiffness is an important regulator of VSMC contractility. We next sought to determine whether VSMC volume, as well as area was enlarged following contractile agonist stimulation on rigid substrates. Quiescent VSMCs were seeded on pliable and rigid hydrogels and stimulated with angiotensin II. Confocal microscopy was used to measure VSMC volume. As previously observed (Ahmed et al., 2022), VSMCs on pliable hydrogels underwent a contractile response following angiotensin II stimulation, decreasing in cell area but displaying no change in volume (**Figure 3a-c**). In contrast, angiotensin II stimulation of VSMCs on rigid hydrogels resulted in both cell area and volume enlargement, indicative of a hypertrophic response (**Figure 3a-c**). On both stiffnesses of hydrogel, angiotensin II stimulated VSMCs displayed a positive correlation between cell area and volume (**Figure 3d**). Linear regression revealed that VSMC area and volume displayed a moderate relationship with no significant difference between the slopes.

### **3.3 Isolated smooth muscle cells generate enhanced traction stress on rigid substrates following contractile agonist stimulation.**

Based on morphological changes, stimulation with a contractile agonist promotes VSMC contraction on pliable hydrogels, whereas those on rigid hydrogels undergo hypertrophy. Previous studies have shown that matrix rigidity promotes increased VSMC traction stress generation (Sazonova et al., 2015; Xie et al., 2018; Petit et al., 2019). However, others demonstrate that increased traction stress generation correlates with a reduction in VSMC area (Nolasco et al., 2020; Ahmed et al., 2022). To determine whether angiotensin II stimulated VSMCs seeded on rigid hydrogels generated enhanced traction stresses, we next performed traction force microscopy. Analysis revealed that VSMCs seeded on rigid hydrogels generated greater maximal and total traction stress following angiotensin II stimulation, compared to their counterparts on pliable hydrogels (**Figure 4a-c**). As cells generate actomyosin derived traction forces, deformational stresses are also placed upon the cell membrane. Microtubules exist in a mechanical balance with actomyosin activity, serving as compression bearing struts capable of resisting deformational stresses (Stamenović, 2005; Brangwynne et al., 2006; Johnson et al., 2021). This relationship is defined by the tensegrity model which predicts that microtubule destabilisation will lead to greater actomyosin derived force generation (Stamenović, 2005).

As VSMCs on rigid hydrogels generate enhanced traction stresses, we predicted that decreased microtubule stability may contribute to increased traction stress generation. To test this, we performed a cold-stable microtubule assay on isolated VSMCs in the presence or absence of angiotensin II stimulation. Upon exposure to cold temperatures, microtubules readily undergo catastrophe, with only stabilised microtubule filaments remaining. After clearing the tubulin monomers, the number of stabilised microtubules can be counted (Ochoa et al., 2011). Analysis revealed that on pliable hydrogels, angiotensin II stimulation had no effect on microtubule stability (**Figure 4d & e**). In comparing microtubule stability between pliable and rigid hydrogels, microtubule stability was found to increase in unstimulated VSMCs that were seeded on stiffer substrates (**Figure 4d & e**). However, following angiotensin II stimulation this enhanced stability was lost, with angiotensin II stimulated VSMCs seeded on rigid hydrogels displaying similar levels of microtubule stability as cells seeded on pliable hydrogels (**Figure 4d & e**).

### 3.4 Microtubule destabilisation leads to isolated smooth muscle cell hypertrophy following contractile agonist stimulation.

The above data shows that on rigid substrates, angiotensin II stimulated VSMCs to undergo a hypertrophic response that is accompanied by an increase in traction force generation and a decrease in microtubule stability. We hypothesised that the loss of microtubule stability was driving VSMC hypertrophy on rigid hydrogels. Quiescent VSMCs were seeded onto pliable and rigid hydrogels and pre-treated with increasing concentrations of microtubule stabilisers prior to angiotensin II stimulation. Treatment with two microtubule stabilisers, paclitaxel or epothilone B, had no effect on the contractile response of VSMCs seeded on pliable hydrogels (**Figure 5a, b, d-f & h**). Meanwhile, increasing concentrations of either microtubule stabiliser was sufficient to prevent the increase in VSMC area observed following angiotensin II stimulation on rigid hydrogels (**Figure 5a, c-e, g & h**). We next hypothesised that microtubule destabilisation would trigger the hypertrophic response in angiotensin II stimulated VSMCs on pliable hydrogels. VSMCs were pre-treated with increasing concentrations of the microtubule destabilisers colchicine or nocodazole, and then stimulated with angiotensin II. On pliable hydrogels, VSMCs treated with either colchicine or nocodazole displayed increased cell area following angiotensin II stimulation (**Figure 6a, b, d-f & h**). In contrast, treatment with the microtubule destabilisers had no effect on VSMCs seeded on rigid hydrogels (**Figure 6a, c-e, g & h**). All microtubule targeting agents were used at concentrations that did not cause cell death, as confirmed through a viability assay for concentrations of epothilone B and nocodazole (**Supplementary Figure S1**) or previously for paclitaxel and colchicine (Ahmed et al., 2022). EC<sub>50</sub> values for all compounds are presented in **Supplementary Table 1**.

Having determined that microtubule stability regulated changes in VSMC area, we then sought to confirm its regulation of VSMC volume. Quiescent VSMCs were pre-treated with paclitaxel (1 nM) or colchicine (100 nM), concentrations that altered both VSMC area (**Figure 5a-d, 6a-d**) and caused a detectable change in the number of cold-stable microtubules (**Supplementary Figure S2**). Following pre-treatment, VSMCs were stimulated with angiotensin II and confocal microscopy was used to assess changes in cell volume. Treatment with the microtubule stabiliser paclitaxel had no effect on the volume of VSMCs seeded on pliable hydrogels (**Figure 7a-c**). Whereas, on rigid hydrogels, microtubule stabilisation prevented the angiotensin II induced expansion of VSMC volume (**Figure 7a-c**). Finally, microtubule destabilisation, via colchicine pre-treatment, increased VSMC volume on pliable hydrogels following angiotensin II stimulation. No further increase in VSMC volume following microtubule destabilisation was observed in VSMCs seeded on rigid hydrogels (**Figure 7d-f**).

#### *Discussion and Conclusions*

Our understanding of the mechanisms driving VSMC dysfunction and its contribution to decreased aortic compliance in ageing and CV disease remains limited. Progress has been hindered by a lack of easy to use, *in vitro* tools through which disease causing pathways can be delineated. We set out to validate an assay for identifying novel regulators of VSMC response to matrix rigidity by comparing their response on pliable vs rigid hydrogels. The physical stiffnesses of these hydrogels (pliable 12 kPa, rigid 72 kPa) were selected to mimic the respective stiffnesses of a healthy vs aged/diseased aorta (Hayenga et al., 2011; Tracqui et al.,

2011; Minaisah et al., 2016; Rezvani-Sharif et al., 2019). We show that contractile agonist stimulation of quiescent VSMCs on pliable or rigid hydrogels results in a differential response; VSMCs on pliable hydrogels decreased in area as they contracted, whereas increased cell area was observed in VSMCs on rigid hydrogels. Furthermore, on rigid hydrogels, contractile agonist stimulation also promoted an increase in VSMC volume. We therefore identify that enhanced matrix stiffness initiates a hypertrophic response within VSMCs, akin to that seen *in vivo* in response to hypertension (Owens and Schwartz, 1983; Rizzoni et al., 2000; Zhang et al., 2005; Schiffrin, 2012).

In this study, we utilised polyacrylamide hydrogels to develop and validate a new screening approach for identifying novel regulators of matrix rigidity induced VSMC hypertrophy. Polyacrylamide hydrogels are easily fabricated in-house using generic research equipment and skills (Kadow et al., 2007; Caliarì and Burdick, 2016; Minaisah et al., 2016). Previous studies have shown that enhanced matrix stiffness promotes the dedifferentiation of VSMCs, downregulating contractile markers whilst increasing the expression of proliferative genes (Brown et al., 2010; Sazonova et al., 2015; Xie et al., 2018; Nagayama and Nishimiya, 2020). Increased VSMC migration, adhesion and proliferation have also been reported (Wong et al., 2003; Brown et al., 2010; Sazonova et al., 2015; Nagayama and Nishimiya, 2020). Furthermore, in response to matrix stiffness, VSMC reorganise their actin cytoskeleton and generate enhanced traction stresses, a finding we recapitulate in this study (Brown et al., 2010; Sazonova et al., 2015; Petit et al., 2019; Sanyour et al., 2019). Through using our screening assay, we can now identify novel regulators of VSMC contractility and hypertrophy under physiologically or pathologically relevant matrix stiffnesses. This approach is robust enough to identify  $EC_{50}$  and  $IC_{50}$  values for contractile agonists and antagonists. Importantly, we correlated increased VSMC area following angiotensin II stimulation with increased VSMC volume, enabling us to predict potential beneficial or deleterious effects of pharmacological agents prior to confirming their effect on VSMC hypertrophy through 3-dimensional confocal microscopy. Current methods of investigating VSMC hypertrophy generally utilise animal models, i.e. genetic depletion in mice or rat models of hypertension (Owens and Schwartz, 1983; Choi et al., 2019; Bai et al., 2021). Through developing an *in vitro* model, we can now investigate the mechanisms regulating VSMC hypertrophy and the potential of anti-hypertrophic compounds at a greater throughput whilst using a less invasive and more ethical method.

In validating the screening assay, we show that the tensegrity model predicts VSMC behaviour on rigid hydrogels. In this model, microtubules serve as compression bearing struts that resist actomyosin generated strain (Johnson et al., 2021). Healthy VSMC behaviour is therefore a balance between microtubule stability and actomyosin activity; actomyosin activity drives VSMC contraction while the microtubules maintain VSMC morphology and protect against strain induced cellular damage (Stamenović, 2005; Brangwynne et al., 2006). The tensegrity model also predicts that microtubule destabilisation results in increased traction stress generation, a hypothesis previously confirmed by both wire myography and traction force microscopy (Paul et al., 2000; Zhang et al., 2000; Platts et al., 2002; Ahmed et al., 2022). We show that the tensegrity model is driving VSMC hypertrophy in rigid environments, where contractile agonist stimulation triggers microtubule destabilisation. Importantly, treatment with agents that stabilise microtubules blocked VSMC hypertrophy on rigid hydrogels. This suggests that therapeutic pathways that promote microtubule stabilisation may be a potential novel approach to target VSMC hypertrophy in diseased regions. Future research to elucidate the molecular mechanisms linking matrix rigidity to microtubule stability is a critical next step to both increase our understanding of VSMC hypertrophy and for illuminating potential pathways for therapeutic intervention.

Importantly, stabilising microtubules appears to specifically target VSMC hypertrophy, leaving the healthy contractile function intact. This is further confirmed as we show that agents which promote microtubule instability induce VSMC hypertrophy on pliable hydrogels. One of these, colchicine, is currently being researched for its CV benefits. Colchicine treatment has been experimentally shown to protect against endothelial cell dysfunction (Huang et al., 2014; Kajikawa et al., 2019; Zălar et al., 2022), reduce VSMC proliferative and migrational capacities *in vitro* (Zhang et al., 2022), and has been shown to suppress atherosclerotic plaque development in some animal models (Martínez et al., 2018). However, colchicine treatment also increases VSMC isometric force generation in both wire myography and traction force microscopy (Zhang et

al., 2000; Platts et al., 2002; Ahmed et al., 2022), suggesting that colchicine treatment will increase aortic wall rigidity and decrease aortic compliance. In addition, our findings show that colchicine treatment induces VSMC hypertrophy on pliable hydrogels, suggesting that hypertrophy may be an unwanted side effect of any potential colchicine therapy. These findings pave the way for confirmatory studies in *ex vivo* and *in vivo* models, and demonstrate the power of our assay and its potential for identifying side effects of proposed therapies for the treatment of CV and other diseases.

## References

- Ahmed, S., Johnson, Robert.T., Solanki, R., Afewerki, T., Wostear, F., and Warren, Derek.T. (2022). Using Polyacrylamide Hydrogels to Model Physiological Aortic Stiffness Reveals that Microtubules Are Critical Regulators of Isolated Smooth Muscle Cell Morphology and Contractility. *Frontiers in Pharmacology* *13* : 836710.
- Ahmed, S., and Warren, D.T. (2018). Vascular smooth muscle cell contractile function and mechanotransduction. *Vessel Plus* *2* : 36.
- Atkinson, S.J., Gontarczyk, A.M., Alghamdi, A.A., Ellison, T.S., Johnson, R.T., Fowler, W.J., et al. (2018). The  $\beta$ 3-integrin endothelial adhesome regulates microtubule-dependent cell migration. *EMBO Rep* *19* : e44578.
- Bai, L., Kee, H.J., Choi, S.Y., Seok, Y.M., Kim, G.R., Kee, S.-J., et al. (2021). HDAC5 inhibition reduces angiotensin II-induced vascular contraction, hypertrophy, and oxidative stress in a mouse model. *Biomedicine & Pharmacotherapy* *134* : 111162.
- Brangwynne, C.P., MacKintosh, F.C., Kumar, S., Geisse, N.A., Talbot, J., Mahadevan, L., et al. (2006). Microtubules can bear enhanced compressive loads in living cells because of lateral reinforcement. *Journal of Cell Biology* *173* : 733–741.
- Brown, X.Q., Bartolak-Suki, E., Williams, C., Walker, M.L., Weaver, V.M., and Wong, J.Y. (2010). Effect of substrate stiffness and PDGF on the behavior of vascular smooth muscle cells: implications for atherosclerosis. *J Cell Physiol* *225* : 115–122.
- Caliari, S.R., and Burdick, J.A. (2016). A practical guide to hydrogels for cell culture. *Nat Methods* *13* : 405–414.
- Choi, S.Y., Kee, H.J., Sun, S., Seok, Y.M., Ryu, Y., Kim, G.R., et al. (2019). Histone deacetylase inhibitor LMK235 attenuates vascular constriction and aortic remodelling in hypertension. *Journal of Cellular and Molecular Medicine* *23* : 2801–2812.
- Cruickshank, K., Riste, L., Anderson, S.G., Wright, J.S., Dunn, G., and Gosling, R.G. (2002). Aortic Pulse-Wave Velocity and Its Relationship to Mortality in Diabetes and Glucose Intolerance. *Circulation* *106* : 2085–2090.
- Curtis, M.J., Alexander, S., Cirino, G., Docherty, J.R., George, C.H., Giembycz, M.A., et al. (2018). Experimental design and analysis and their reporting II: updated and simplified guidance for authors and peer reviewers. *British Journal of Pharmacology* *175* : 987–993.
- Glasser, S.P., Arnett, D.K., McVeigh, G.E., Finkelstein, S.M., Bank, A.J., Morgan, D.J., et al. (1997). Vascular Compliance and Cardiovascular Disease: A Risk Factor or a Marker? *American Journal of Hypertension* *10* : 1175–1189.
- Halaidych, O.V., Cochrane, A., Hil, F.E. van den, Mummery, C.L., and Orlova, V.V. (2019). Quantitative Analysis of Intracellular Ca<sup>2+</sup> Release and Contraction in hiPSC-Derived Vascular Smooth Muscle Cells. *Stem Cell Reports* *12* : 647–656.
- Hayashi, K., and Naiki, T. (2009). Adaptation and remodeling of vascular wall; biomechanical response to hypertension. *Journal of the Mechanical Behavior of Biomedical Materials* *2* : 3–19.

- Hayenga, H.N., Trache, A., Trzeciakowski, J., and Humphrey, J.D. (2011). Regional atherosclerotic plaque properties in ApoE<sup>-/-</sup> mice quantified by atomic force, immunofluorescence, and light microscopy. *J Vasc Res* *48* : 495–504.
- Huang, C., Cen, C., Wang, C., Zhan, H., and Ding, X. (2014). Synergistic effects of colchicine combined with atorvastatin in rats with hyperlipidemia. *Lipids Health Dis* *13* : 67.
- Johnson, R.T., Solanki, R., and Warren, D.T. (2021). Mechanical programming of arterial smooth muscle cells in health and ageing. *Biophys Rev* *13* : 757–768.
- Kajikawa, M., Higashi, Y., Tomiyama, H., Maruhashi, T., Kurisu, S., Kihara, Y., et al. (2019). Effect of short-term colchicine treatment on endothelial function in patients with coronary artery disease. *International Journal of Cardiology* *281* : 35–39.
- Kadow, C.E., Georges, P.C., Janmey, P.A., and Beningo, K.A. (2007). Polyacrylamide Hydrogels for Cell Mechanics: Steps Toward Optimization and Alternative Uses. In *Methods in Cell Biology*, (Academic Press), pp 29–46.
- Lacolley, P., Regnault, V., and Laurent, S. (2020). Mechanisms of Arterial Stiffening. *Arteriosclerosis, Thrombosis, and Vascular Biology* *40* : 1055–1062.
- Lacolley, P., Regnault, V., Segers, P., and Laurent, S. (2017). Vascular Smooth Muscle Cells and Arterial Stiffening: Relevance in Development, Aging, and Disease. *Physiological Reviews* *97* : 1555–1617.
- Leloup, A.J.A., Van Hove, C.E., De Moudt, S., De Meyer, G.R.Y., De Keulenaer, G.W., and Franssen, P. (2019). Vascular smooth muscle cell contraction and relaxation in the isolated aorta: a critical regulator of large artery compliance. *Physiological Reports* *7* : e13934.
- Li, S., Sims, S., Jiao, Y., Chow, L.H., and Pickering, J.G. (1999). Evidence from a novel human cell clone that adult vascular smooth muscle cells can convert reversibly between noncontractile and contractile phenotypes. *Circ Res* *85* : 338–348.
- Martínez, G.J., Celermajer, D.S., and Patel, S. (2018). The NLRP3 inflammasome and the emerging role of colchicine to inhibit atherosclerosis-associated inflammation. *Atherosclerosis* *269* : 262–271.
- Minisah, R.-M., Cox, S., and Warren, D.T. (2016). The Use of Polyacrylamide Hydrogels to Study the Effects of Matrix Stiffness on Nuclear Envelope Properties. In *The Nuclear Envelope*, S. Shackleton, P. Collas, and E.C. Schirmer, eds. (New York, NY: Springer New York), pp 233–239.
- Mitchell, G.F., Hwang, S.-J., Vasan, R.S., Larson, M.G., Pencina, M.J., Hamburg, N.M., et al. (2010). Arterial Stiffness and Cardiovascular Events. *Circulation* *121* : 505–511.
- Nagayama, K., and Nishimiya, K. (2020). Moderate substrate stiffness induces vascular smooth muscle cell differentiation through cellular morphological and tensional changes. *Biomed Mater Eng* *31* : 157–167.
- Nolasco, P., Fernandes, C.G., Ribeiro-Silva, J.C., Oliveira, P.V.S., Sacrini, M., Brito, I.V. de, et al. (2020). Impaired vascular smooth muscle cell force-generating capacity and phenotypic deregulation in Marfan Syndrome mice. *Biochimica et Biophysica Acta (BBA) - Molecular Basis of Disease* *1866* : 165587.
- Ochoa, C.D., Stevens, T., and Balczon, R. (2011). Cold exposure reveals two populations of microtubules in pulmonary endothelia. *Am J Physiol Lung Cell Mol Physiol* *300* : L132–L138.
- Owens, G.K., and Schwartz, S.M. (1983). Vascular smooth muscle cell hypertrophy and hyperploidy in the Goldblatt hypertensive rat. *Circulation Research* *53* : 491–501.
- Paul, R.J., Bowman, P.S., and Kolodney, M.S. (2000). Effects of microtubule disruption on force, velocity, stiffness and [Ca<sup>2+</sup>]<sub>i</sub> in porcine coronary arteries. *American Journal of Physiology-Heart and Circulatory Physiology* *279* : H2493–H2501.

- Petit, C., Guignandon, A., and Avril, S. (2019). Traction Force Measurements of Human Aortic Smooth Muscle Cells Reveal a Motor-Clutch Behavior. *Molecular and Cellular Biomechanics*.
- Platts, S.H., Martinez-Lemus, L.A., and Meininger, G.A. (2002). Microtubule-Dependent Regulation of Vasomotor Tone Requires Rho-Kinase. *JVR* *39* : 173–182.
- Porter, L., Minaisah, R.-M., Ahmed, S., Ali, S., Norton, R., Zhang, Q., et al. (2020). SUN1/2 Are Essential for RhoA/ROCK-Regulated Actomyosin Activity in Isolated Vascular Smooth Muscle Cells. *Cells* *9* : 132.
- Qiu, H., Zhu, Y., Sun, Z., Trzeciakowski, J.P., Gansner, M., Depre, C., et al. (2010). Short Communication: Vascular Smooth Muscle Cell Stiffness As a Mechanism for Increased Aortic Stiffness With Aging. *Circulation Research* *107* : 615–619.
- Ragnauth, C.D., Warren, D.T., Liu, Y., McNair, R., Tajsic, T., Figg, N., et al. (2010). Prelamin A Acts to Accelerate Smooth Muscle Cell Senescence and Is a Novel Biomarker of Human Vascular Aging. *Circulation* *121* : 2200–2210.
- Rezvani-Sharif, A., Tafazzoli-Shadpour, M., and Avolio, A. (2019). Progressive changes of elastic moduli of arterial wall and atherosclerotic plaque components during plaque development in human coronary arteries. *Med Biol Eng Comput* *57* : 731–740.
- Rizzoni, D., Porteri, E., Guefi, D., Piccoli, A., Castellano, M., Pasini, G., et al. (2000). Cellular Hypertrophy in Subcutaneous Small Arteries of Patients With Renovascular Hypertension. *Hypertension* *35* : 931–935.
- Safar, M.E., Henry, O., and Meaume, S. (2002). Aortic Pulse Wave Velocity: An Independent Marker of Cardiovascular Risk. *The American Journal of Geriatric Cardiology* *11* : 295–304.
- Sanyour, H.J., Li, N., Rickel, A.P., Childs, J.D., Kinser, C.N., and Hong, Z. (2019). Membrane cholesterol and substrate stiffness co-ordinate to induce the remodelling of the cytoskeleton and the alteration in the biomechanics of vascular smooth muscle cells. *Cardiovasc Res* *115* : 1369–1380.
- Sazonova, O.V., Isenberg, B.C., Herrmann, J., Lee, K.L., Purwada, A., Valentine, A.D., et al. (2015). Extracellular matrix presentation modulates vascular smooth muscle cell mechanotransduction. *Matrix Biology* *41* : 36–43.
- Sazonova, O.V., Lee, K.L., Isenberg, B.C., Rich, C.B., Nugent, M.A., and Wong, J.Y. (2011). Cell-Cell Interactions Mediate the Response of Vascular Smooth Muscle Cells to Substrate Stiffness. *Biophysical Journal* *101* : 622–630.
- Schiffirin, E.L. (2012). Vascular Remodeling in Hypertension. *Hypertension* *59* : 367–374.
- Schindelin, J., Arganda-Carreras, I., Frise, E., Kaynig, V., Longair, M., Pietzsch, T., et al. (2012). Fiji: an open-source platform for biological-image analysis. *Nat Methods* *9* : 676–682.
- Sehgel, N.L., Sun, Z., Hong, Z., Hunter, W.C., Hill, M.A., Vatner, D.E., et al. (2015a). Augmented Vascular Smooth Muscle Cell Stiffness and Adhesion When Hypertension Is Superimposed on Aging. *Hypertension* *65* : 370–377.
- Sehgel, N.L., Vatner, S.F., and Meininger, G.A. (2015b). “Smooth Muscle Cell Stiffness Syndrome”—Revisiting the Structural Basis of Arterial Stiffness. *Frontiers in Physiology* *6* :
- Sequí-Domínguez, I., Cavero-Redondo, I., Álvarez-Bueno, C., Pozuelo-Carrascosa, D.P., Nuñez de Arenas-Arroyo, S., and Martínez-Vizcaíno, V. (2020). Accuracy of Pulse Wave Velocity Predicting Cardiovascular and All-Cause Mortality. A Systematic Review and Meta-Analysis. *Journal of Clinical Medicine* *9* : 2080.
- Stamenović, D. (2005). Microtubules may harden or soften cells, depending of the extent of cell distension. *Journal of Biomechanics* *38* : 1728–1732.
- Tracqui, P., Broisat, A., Toczek, J., Mesnier, N., Ohayon, J., and Riou, L. (2011). Mapping elasticity moduli of atherosclerotic plaque in situ via atomic force microscopy. *J Struct Biol* *174* : 115–123.

Tsamis, A., Krawiec, J.T., and Vorp, D.A. (2013). Elastin and collagen fibre microstructure of the human aorta in ageing and disease: a review. *Journal of The Royal Society Interface* *10* : 20121004.

Tseng, Q., Duchemin-Pelletier, E., Deshiere, A., Balland, M., Guillou, H., Filhol, O., et al. (2012). Spatial organization of the extracellular matrix regulates cell–cell junction positioning. *PNAS* *109* : 1506–1511.

Wang, L., Qiu, P., Jiao, J., Hirai, H., Xiong, W., Zhang, J., et al. (2017). Yes-Associated Protein Inhibits Transcription of Myocardin and Attenuates Differentiation of Vascular Smooth Muscle Cell from Cardiovascular Progenitor Cell Lineage. *STEM CELLS* *35* : 351–361.

Warren, D.T., Tajsic, T., Porter, L.J., Minaisah, R.M., Cobb, A., Jacob, A., et al. (2015). Nesprin-2-dependent ERK1/2 compartmentalisation regulates the DNA damage response in vascular smooth muscle cell ageing. *Cell Death Differ* *22* : 1540–1550.

Wong, J.Y., Velasco, A., Rajagopalan, P., and Pham, Q. (2003). Directed Movement of Vascular Smooth Muscle Cells on Gradient-Compliant Hydrogels. *Langmuir* *19* : 1908–1913.

Xie, S.-A., Zhang, T., Wang, J., Zhao, F., Zhang, Y.-P., Yao, W.-J., et al. (2018). Matrix stiffness determines the phenotype of vascular smooth muscle cell in vitro and in vivo: Role of DNA methyltransferase 1. *Biomaterials* *155* : 203–216.

Zălar, D.-M., Pop, C., Buzdugan, E., Kiss, B., Ștefan, M.-G., Ghibu, S., et al. (2022). Effects of Colchicine in a Rat Model of Diet-Induced Hyperlipidemia. *Antioxidants* *11* : 230.

Zhang, D., Jin, N., Rhoades, R.A., Yancey, K.W., and Swartz, D.R. (2000). Influence of microtubules on vascular smooth muscle contraction. *J Muscle Res Cell Motil* *21* : 293–300.

Zhang, F., He, Q., Qin, C.H., Little, P.J., Weng, J., and Xu, S. (2022). Therapeutic potential of colchicine in cardiovascular medicine: a pharmacological review. *Acta Pharmacol Sin* *43* : 2173–2190.

Zhang, Y., Griendling, K.K., Dikalova, A., Owens, G.K., and Taylor, W.R. (2005). Vascular Hypertrophy in Angiotensin II–Induced Hypertension Is Mediated by Vascular Smooth Muscle Cell–Derived H<sub>2</sub>O<sub>2</sub>. *Hypertension* *46* : 732–737.

Zhong, Q., Hu, M.-J., Cui, Y.-J., Liang, L., Zhou, M.-M., Yang, Y.-W., et al. (2018). Carotid–Femoral Pulse Wave Velocity in the Prediction of Cardiovascular Events and Mortality: An Updated Systematic Review and Meta-Analysis. *Angiology* *69* : 617–629.

Zieman, S.J., Melenovsky, V., and Kass, D.A. (2005). Mechanisms, Pathophysiology, and Therapy of Arterial Stiffness. *Arteriosclerosis, Thrombosis, and Vascular Biology* *25* : 932–943.

### Figure Legends

#### Figure 1. VSMC response to contractile agonist stimulation is matrix stiffness dependent.

(a) Representative images of isolated VSMCs cultured on 12 or 72 kPa polyacrylamide hydrogels treated with increasing concentrations of angiotensin II (0.01 – 100  $\mu$ M) for 30 minutes. Actin cytoskeleton (purple) and Lamin A/C labelled nuclei (green). Scale bar = 100  $\mu$ m. VSMC area on (b) 12 kPa and (c) 72 kPa hydrogels representative of 5 independent experiments with [?]158 cells analysed per condition. Significance determined using a one-way ANOVA followed by Tukey’s test. (d) Comparison of VSMC response to angiotensin II on 12 and 72 kPa hydrogels. Data is expressed as the mean of the means calculated from 5 independent experiments; significance determined using a two-way ANOVA followed by Sidak’s test. (e) Representative images of isolated VSMCs cultured on 12 or 72 kPa polyacrylamide hydrogels treated with increasing concentrations of carbachol (0.01 – 100  $\mu$ M) for 30 minutes. Actin cytoskeleton (purple) and Lamin A/C labelled nuclei (green). Scale bar = 100  $\mu$ m. VSMC area on (f) 12 kPa and (g) 72 kPa hydrogels representative of 5 independent experiments with [?]149 cells analysed per condition. Significance determined using a one-way ANOVA followed by Tukey’s test. (h) Comparison of VSMC response to carbachol on 12 and 72 kPa hydrogels. Data is expressed as the mean of the means calculated from 5 independent experiments;

significance determined using a two-way ANOVA followed by Sidak's test. ( $* = p < 0.05$  , error bars represent  $\pm$  SEM).

**Figure 2. VSMC response to contractile agonist stimulation is blocked by receptor antagonisation.** (a) Representative images of isolated VSMCs cultured on 12 or 72 kPa polyacrylamide hydrogels treated with angiotensin II (10  $\mu$ M) for 30 minutes in the presence of increasing concentrations of irbesartan (0.023 – 230 nM). Actin cytoskeleton (purple) and Lamin A/C labelled nuclei (green). Scale bar = 100  $\mu$ m. VSMC area on (b) 12 kPa and (c) 72 kPa hydrogels representative of 5 independent experiments with [?]97 cells analysed per condition. Significance determined using a one-way ANOVA followed by Tukey's test. (d) Comparison of VSMC response to angiotensin II in the presence of irbesartan on 12 and 72 kPa hydrogels. Data is expressed as the mean of the means calculated from 5 independent experiments; significance determined using a two-way ANOVA followed by Sidak's test. (e) Representative images of isolated VSMCs cultured on 12 or 72 kPa polyacrylamide hydrogels treated with carbachol (10  $\mu$ M) for 30 minutes in the presence of increasing concentrations of atropine (0.038 – 380 nM). Actin cytoskeleton (purple) and Lamin A/C labelled nuclei (green). Scale bar = 100  $\mu$ m. VSMC area on (f) 12 kPa and (g) 72 kPa hydrogels representative of 5 independent experiments with [?]93 cells analysed per condition. Significance determined using a one-way ANOVA followed by Tukey's test. (h) Comparison of VSMC response to carbachol in the presence of atropine on 12 and 72 kPa hydrogels. Data is expressed as the mean of the means calculated from 5 independent experiments; significance determined using a two-way ANOVA followed by Sidak's test. ( $* = p < 0.05$  , error bars represent  $\pm$  SEM).

**Figure 3. VSMC undergo a hypertrophic response on rigid substrates following angiotensin II stimulation.** (a) Representative images of isolated VSMCs cultured on 12 or 72 kPa polyacrylamide hydrogels in the presence or absence of angiotensin II (AngII) (10  $\mu$ M). Actin cytoskeleton (purple) and Lamin A/C labelled nuclei (green). Top – Representative XY images of VSMC area, scale bar = 100  $\mu$ m. Bottom – Representative XZ images of VSMC height, scale bar = 20  $\mu$ m. (b) VSMC area and (c) volume, representative of 5 independent experiments with [?]82 cells analysed per condition. Significance determined using a one-way ANOVA followed by Sidak's test. (d) Correlation between area and volume in angiotensin II stimulated VSMCs on 12 and 72 kPa hydrogels. Linear regression was used to determine  $R^2$  values and differences between the slopes. ( $* = p < 0.05$  , error bars represent  $\pm$  SEM).

**Figure 4. VSMCs generate enhanced traction stress on rigid substrates following angiotensin II stimulation.** (a) Representative phase images and bead displacement heat maps of angiotensin II (AngII) (10  $\mu$ M) stimulated VSMCs cultured on 12 or 72 kPa polyacrylamide hydrogels. Scale bar = 20  $\mu$ m. (b) maximum and (c) total traction stress generation, representative of 5 independent experiments, with [?]38 cells analysed per condition. (d) Representative images of isolated VSMCs seeded on 12 or 72 kPa polyacrylamide hydrogels in the presence or absence of AngII (10  $\mu$ M) stimulation. Cold-stable microtubules, ( $\alpha$ -tubulin, aqua) and nuclei (DAPI, blue). Scale bar = 50  $\mu$ m. (e) number of cold-stable microtubules per cell, representative of 5 independent experiments, with [?]81 cells analysed per condition; significance determined using a two-way ANOVA followed by Sidak's test. ( $* = p < 0.05$  , error bars represent  $\pm$  SEM).

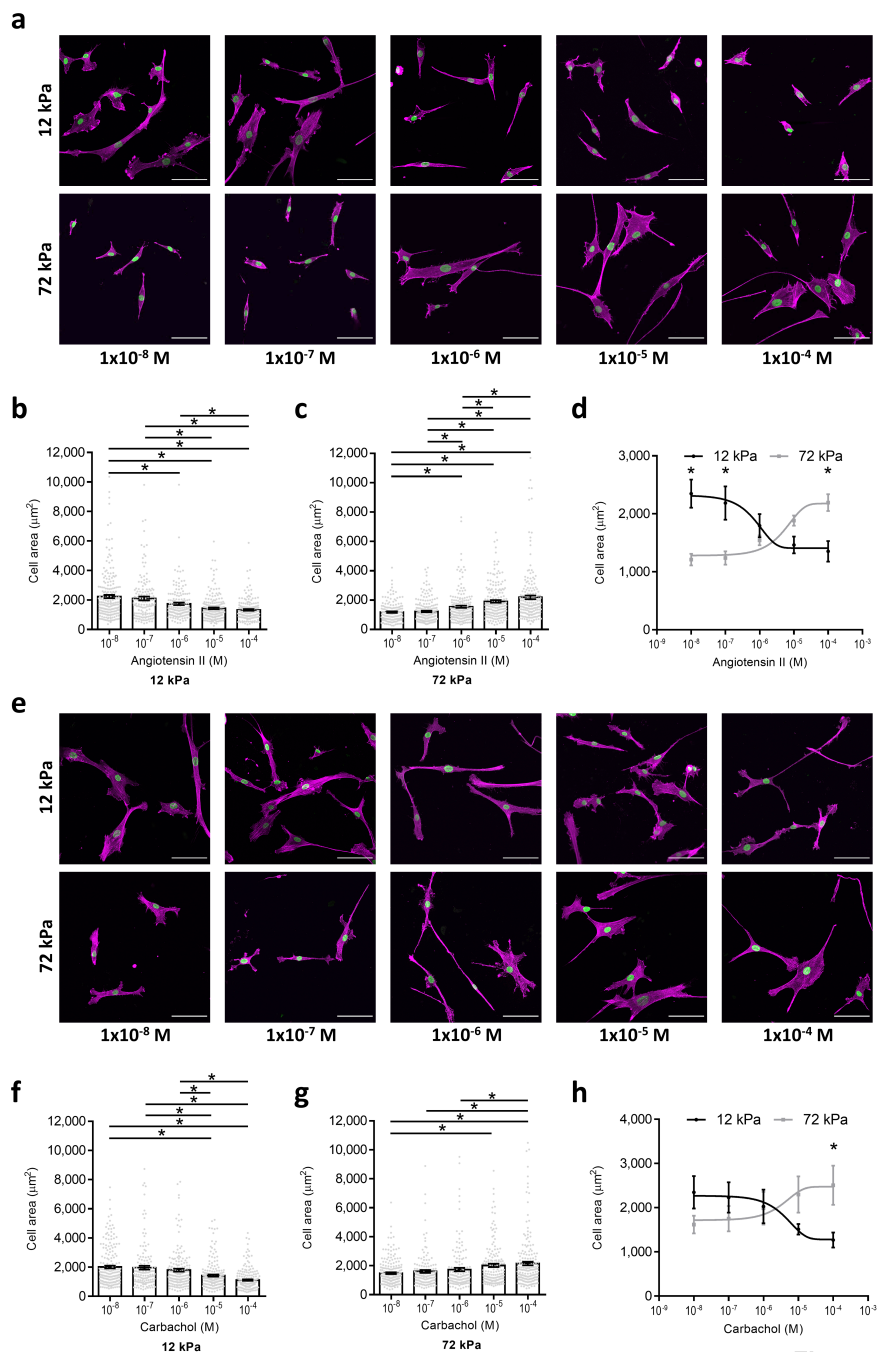
**Figure 5. Microtubule stabilisation prevents VSMC hypertrophy on rigid substrates following angiotensin II stimulation.** (a) Representative images of isolated VSMCs cultured on 12 or 72 kPa polyacrylamide hydrogels pre-treated with increasing concentrations of paclitaxel (0.001 – 10 nM) prior to angiotensin II (10  $\mu$ M) stimulation. Actin cytoskeleton (purple) and Lamin A/C labelled nuclei (green). Scale bar = 100  $\mu$ m. VSMC area on (b) 12 kPa and (c) 72 kPa hydrogels representative of 5 independent experiments with [?]100 cells analysed per condition. Significance determined using a one-way ANOVA followed by Tukey's test. (d) Comparison of VSMC response to paclitaxel pre-treatment on 12 and 72 kPa hydrogels. Data is expressed as the mean of the means calculated from 5 independent experiments; significance determined using a two-way ANOVA followed by Sidak's test. (e) Representative images of isolated VSMCs cultured on 12 or 72 kPa polyacrylamide hydrogels pre-treated with increasing concentrations of epothilone B (0.001 – 10 nM) prior to angiotensin II (10  $\mu$ M) stimulation. Actin cytoskeleton (purple) and Lamin A/C labelled nuclei (green). Scale bar = 100  $\mu$ m. VSMC area on (f) 12 kPa and (g) 72 kPa hydrogels

representative of 5 independent experiments with [?]<sup>53</sup> cells analysed per condition. Significance determined using a one-way ANOVA followed by Tukey’s test. (h) Comparison of VSMC response to epothilone B pre-treatment on 12 and 72 kPa hydrogels. Data is expressed as the mean of the means calculated from 5 independent experiments; significance determined using a two-way ANOVA followed by Sidak’s test. (n.s. = *non-significant* , \* =  $p < 0.05$  , error bars represent  $\pm$  SEM).

**Figure 6. Microtubule destabilisation triggers VSMC hypertrophy on pliable substrates following angiotensin II stimulation.** (a) Representative images of isolated VSMCs cultured on 12 or 72 kPa polyacrylamide hydrogels pre-treated with increasing concentrations of colchicine (0.1 – 1000 nM) prior to angiotensin II (10  $\mu$ M) stimulation. Actin cytoskeleton (purple) and Lamin A/C labelled nuclei (green). Scale bar = 100  $\mu$ m. VSMC area on (b) 12 kPa and (c) 72 kPa hydrogels representative of 5 independent experiments with [?]<sup>79</sup> cells analysed per condition. Significance determined using a one-way ANOVA followed by Tukey’s test. (d) Comparison of VSMC response to colchicine pre-treatment on 12 and 72 kPa hydrogels. Data is expressed as the mean of the means calculated from 5 independent experiments; significance determined using a two-way ANOVA followed by Sidak’s test. (e) Representative images of isolated VSMCs cultured on 12 or 72 kPa polyacrylamide hydrogels pre-treated with increasing concentrations of nocodazole (0.001 – 10 nM) prior to angiotensin II (10  $\mu$ M) stimulation. Actin cytoskeleton (purple) and Lamin A/C labelled nuclei (green). Scale bar = 100  $\mu$ m. VSMC area on (f) 12 kPa and (g) 72 kPa hydrogels representative of 5 independent experiments with [?]<sup>58</sup> cells analysed per condition. Significance determined using a one-way ANOVA followed by Tukey’s test. (h) Comparison of VSMC response to nocodazole pre-treatment on 12 and 72 kPa hydrogels. Data is expressed as the mean of the means calculated from 5 independent experiments; significance determined using a two-way ANOVA followed by Sidak’s test. (n.s. = *non-significant* , \* =  $p < 0.05$  , error bars represent  $\pm$  SEM).

**Figure 7. VSMC hypertrophy is regulated by microtubule stability.** (a) Representative images of isolated VSMCs cultured on 12 or 72 kPa polyacrylamide hydrogels pre-treated with paclitaxel (1 nM), prior to angiotensin II (10  $\mu$ M) stimulation. Actin cytoskeleton (purple) and Lamin A/C labelled nuclei (green). Top – Representative XY images of VSMC area, scale bar = 100  $\mu$ m. Bottom – Representative XZ images of VSMC height, scale bar = 20  $\mu$ m. (b) VSMC area and (c) volume, representative of 5 independent experiments with [?]<sup>114</sup> cells analysed per condition. (d) Representative images of isolated VSMCs cultured on 12 or 72 kPa polyacrylamide hydrogels pre-treated with colchicine (100 nM), prior to angiotensin II (10  $\mu$ M) stimulation. Actin cytoskeleton (purple) and Lamin A/C labelled nuclei (green). Top – Representative XY images of VSMC area, scale bar = 100  $\mu$ m. Bottom – Representative XZ images of VSMC height, scale bar = 20  $\mu$ m. (e) VSMC area and (f) volume, representative of 5 independent experiments with [?]<sup>113</sup> cells analysed per condition. Significance determined using a one-way ANOVA followed by Sidak’s test. (\* =  $p < 0.05$  , error bars represent  $\pm$  SEM).

**Graphical Abstract. Microtubule stability regulates VSMC response to contractile agonist stimulation.** Following contractile agonist stimulation, isolated VSMCs seeded on pliable substrates undergo a contractile response, decreasing in cell area whilst maintaining a consistent volume. VSMCs seeded on rigid substrates fail to undergo a contractile response following contractile agonist stimulation and instead undergo a hypertrophic response, increasing in area and volume. VSMC hypertrophy can be prevented on rigid substrates through microtubule stabilisation. In VSMCs seeded on pliable substrates, microtubule destabilisation inhibits the contractile response and promotes VSMC hypertrophy.



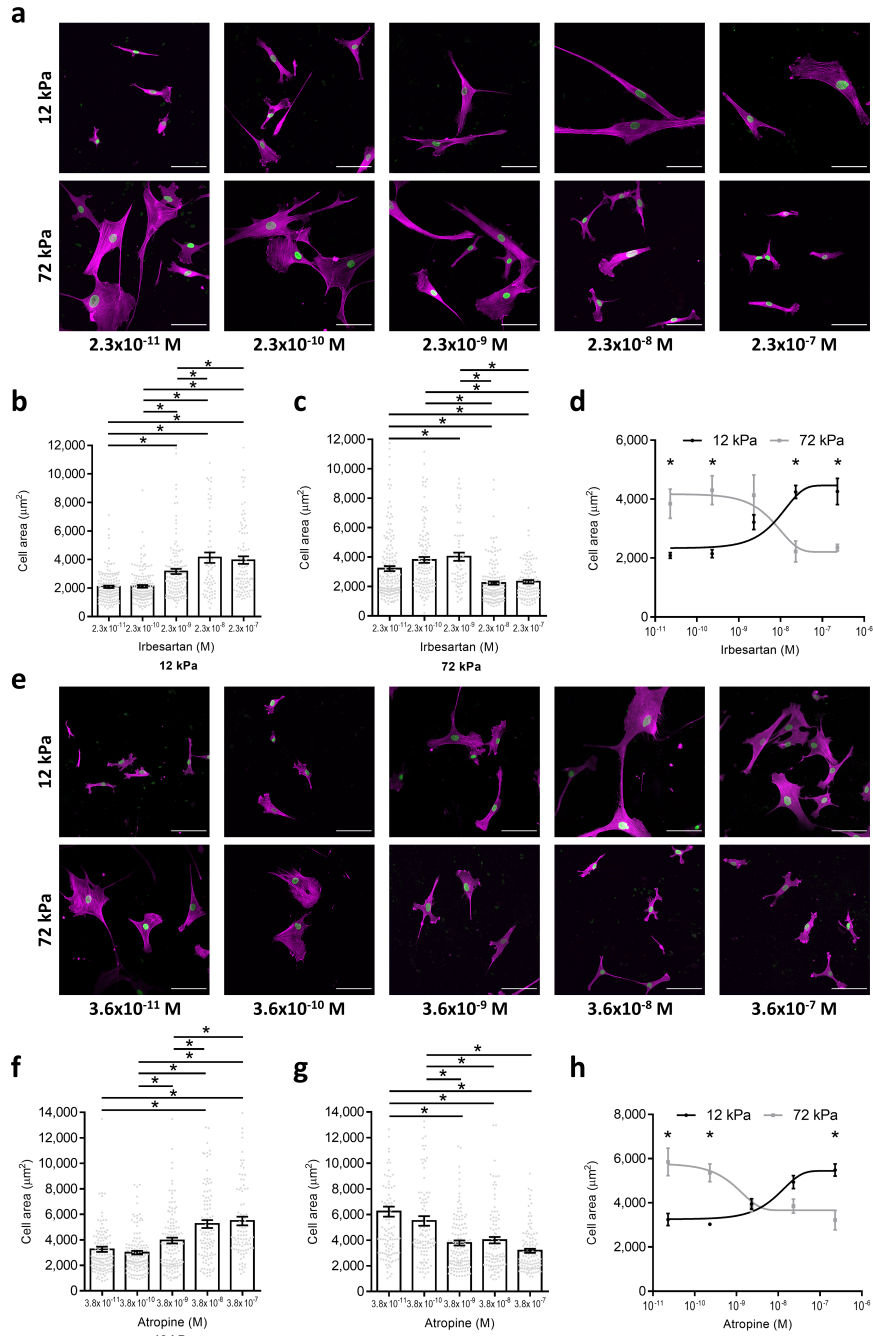


**Figure 2**

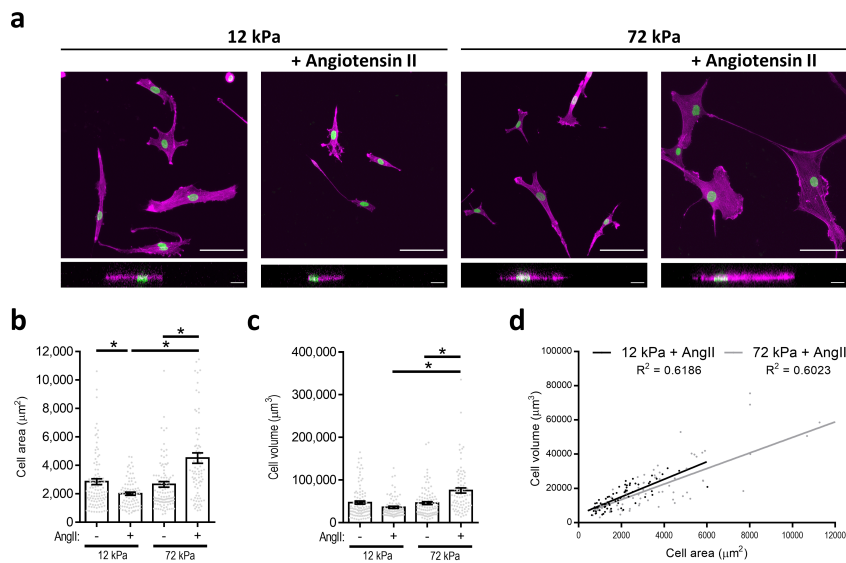


**Figure 3**

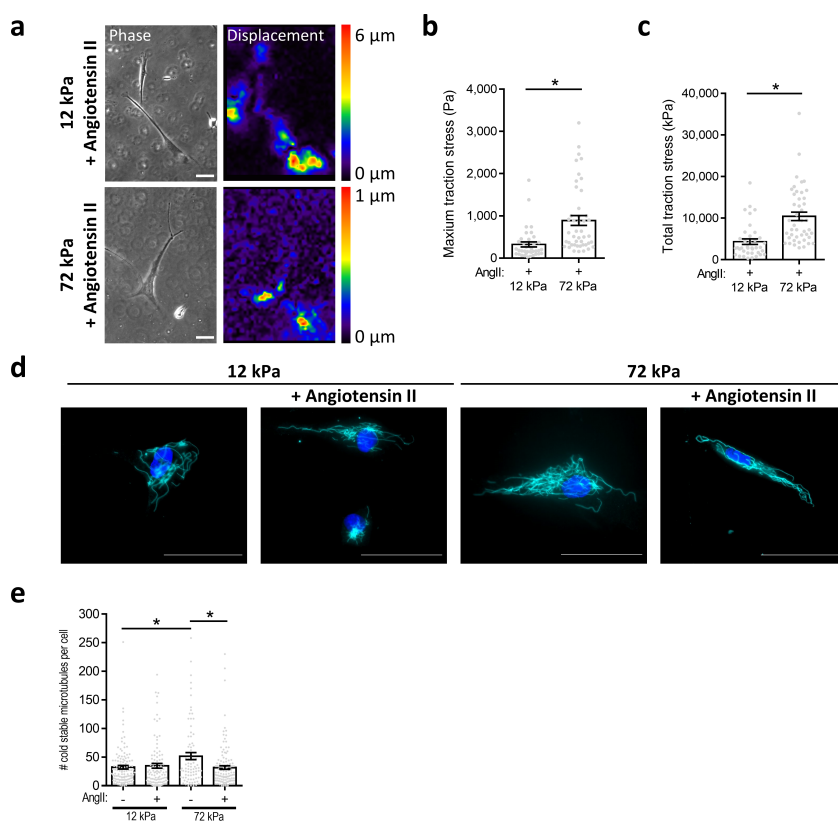


**Figure 4**

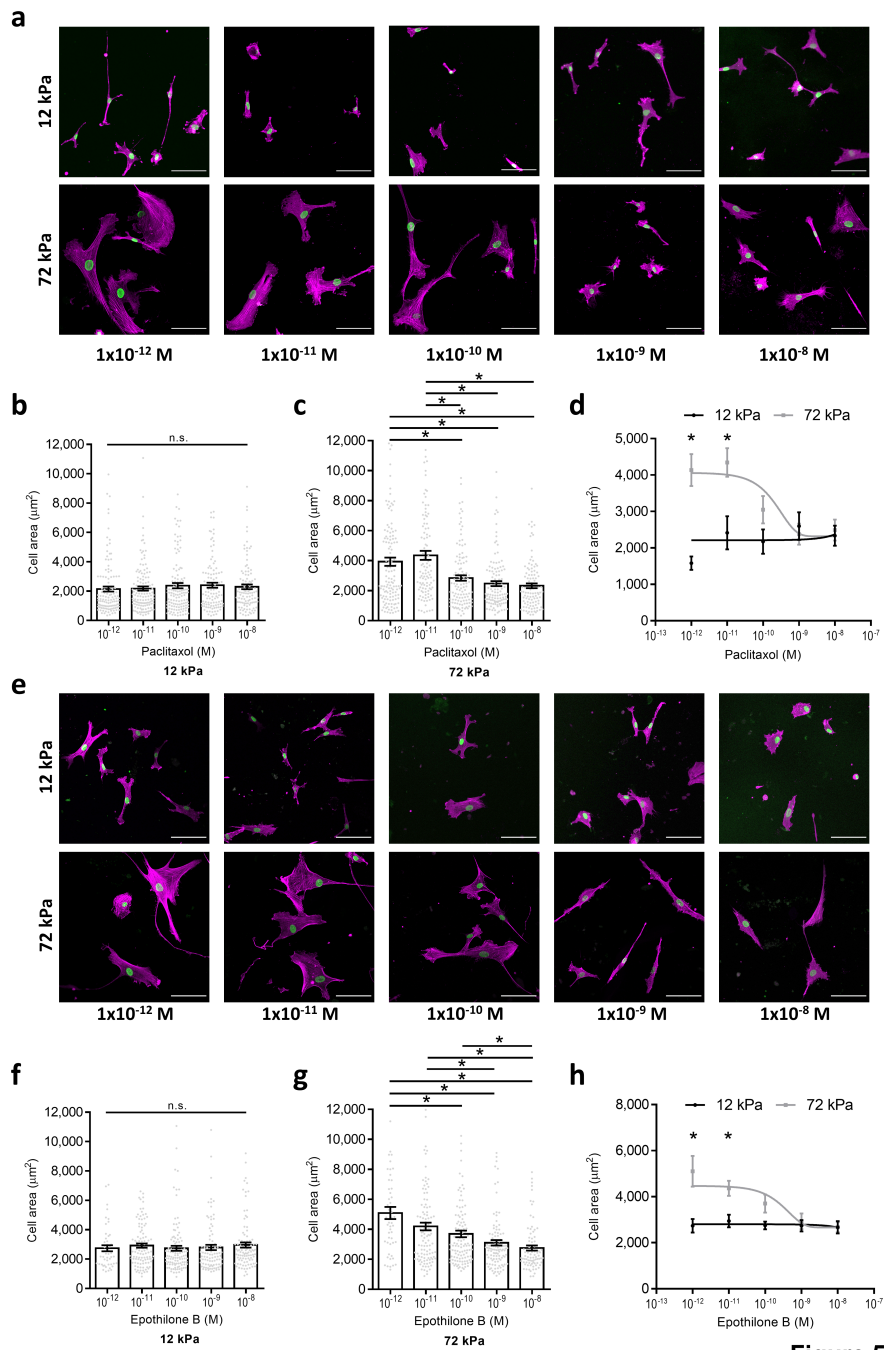


**Figure 5**

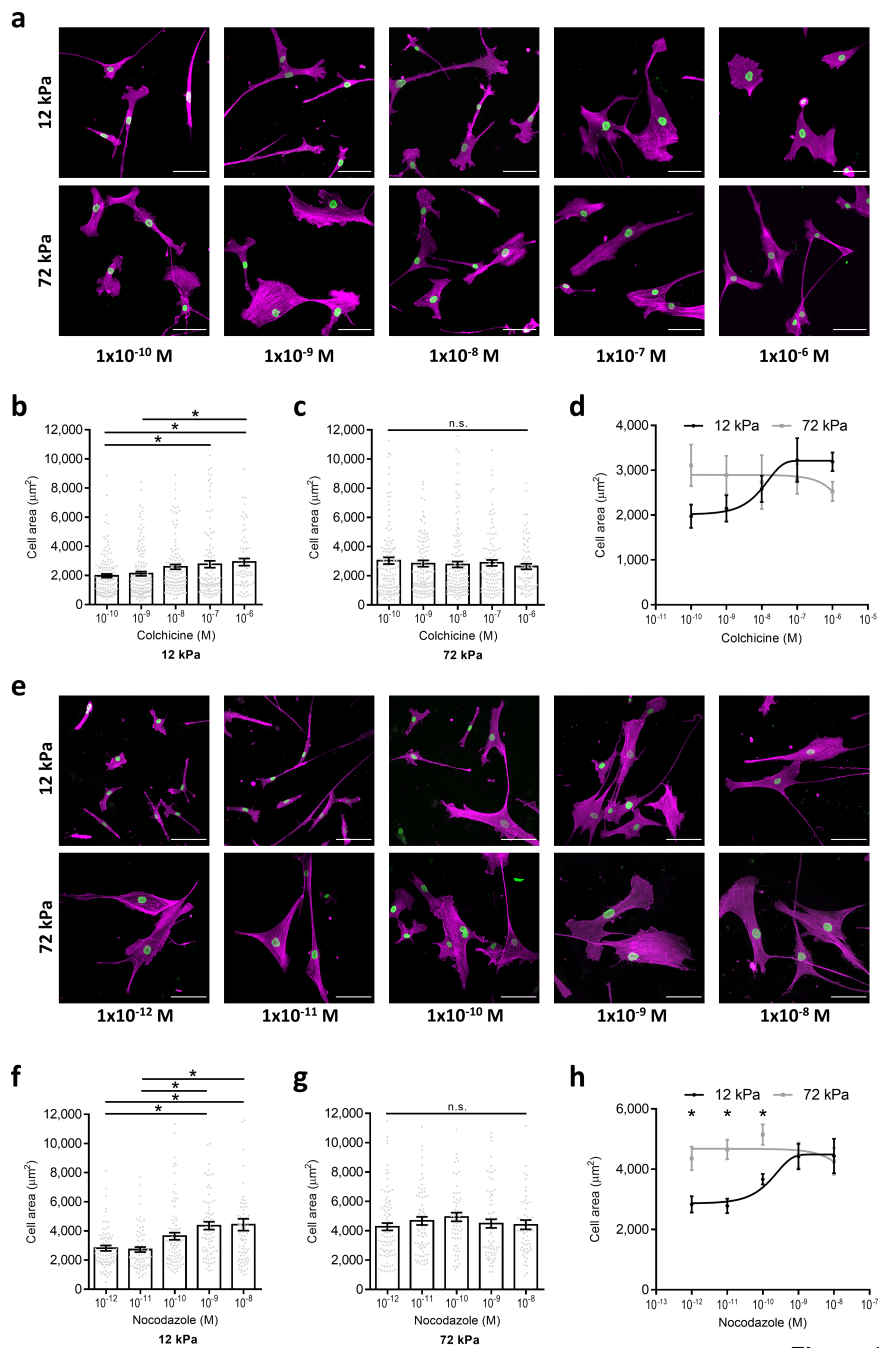


**Figure 6**

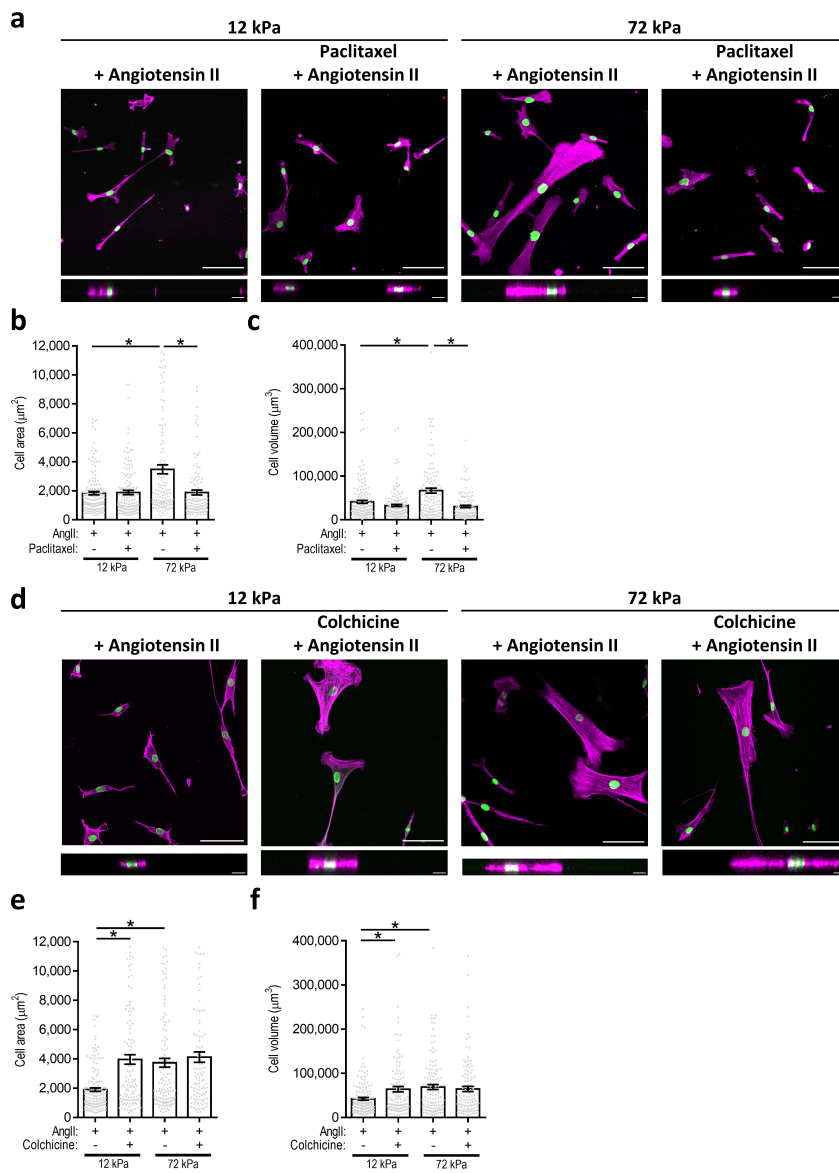


Figure 7